

Actively Coupled Sensor Configuration and Planning in Unknown Dynamic Environments

Prakash Poudel*, Jeffrey DesRoches*, and Raghendra V. Cowlagi†

Abstract—We address the problem of path-planning for an autonomous mobile vehicle, called the ego vehicle, in an unknown and time-varying environment. The objective is for the ego vehicle to minimize exposure to a spatiotemporally-varying unknown scalar field called the threat field. Noisy measurements of the threat field are provided by a network of mobile sensors. We address the problem of optimally configuring (placing) these sensors in the environment. To this end, we propose sensor reconfiguration by maximizing a reward function composed of three different elements. First, the reward includes an information measure that we call context-relevant mutual information (CRMI). Unlike typical sensor placement techniques that maximize mutual information of the measurements and environment state, CRMI directly quantifies uncertainty reduction in the ego path cost while it moves in the environment. Therefore, the CRMI introduces active coupling between the ego vehicle and the sensor network. Second, the reward includes a penalty on the distances traveled by the sensors. Third, the reward includes a measure of proximity of the sensors to the ego vehicle. Although we do not consider communication issues in this paper, such proximity is of relevance for future work that addresses communications between the sensors and the ego vehicle. We illustrate and analyze the proposed technique via numerical simulations.

I. INTRODUCTION

Many envisioned applications of autonomous mobile agents, such as emergency first response after natural disasters, involve operations in dynamic and uncertain environments. In such applications, an autonomous agent may need to navigate through adverse environmental conditions, to which we would like to minimize exposure. We refer to these adverse conditions in aggregate as a *threat field*. The threat field is a spatiotemporally-varying scalar field that represents unfavorable conditions such as extreme weather, harmful chemical substances, or radiation. The agent may need to traverse the environment while balancing the competing objectives of reducing exposure to the threat and reducing mission completion time. In the rest of this paper, we refer to this agent as the *ego vehicle*.

The ego vehicle is supported by a spatially distributed network of mobile sensors. These sensors collect real-time data of the threat field, which may be used by the ego vehicle. In applications such as emergency first response, the availability of mobile sensors, such as unmanned aerial vehicles (UAVs), to gather information over large areas may be limited. With this motivation, we focus on the problem of path-planning for the ego vehicle using a minimal number of sensor measurements.

This problem is naturally related to several different disciplines in the literature including path-planning under uncertainty and state estimation. Utilizing sensor data from a mobile sensor network also introduces the problem of optimal sensor placement, which is necessary to ensure that ego vehicle has adequate information about the threat field with as few measurements as possible.

Classical approaches to path-planning include cell decomposition, probabilistic roadmaps, and artificial potential field techniques [1], [2]. Dijkstra’s algorithm, A*, and their variants are branch-and-bound optimization methods that use heuristics to systematically explore the search space and identify the shortest path. While classical path-planning methods are powerful, they are inherently limited by the accuracy of the environment’s available information. An accurate representation of the environment is difficult if the environment’s states or dynamics are unknown. Learning-based approaches, particularly deep reinforcement learning (RL) [3], [4] are gaining attention for their ability to handle complex and uncertain environments.

Sensor data are always noisy and often incomplete, and therefore it is necessary to apply probabilistic estimation techniques to obtain accurate information. The literature on estimation includes various Bayesian techniques, such as the Kalman filter [5], maximum likelihood estimator [6], and Bayesian filter [7]. The use of the extended Kalman filter (EKF), the unscented Kalman filter (UKF) [8], or the particle filter [9] is prevalent for nonlinear dynamical systems.

Various sensor placement strategies have been employed depending on the type of application and parameters that need to be measured. Greedy approaches that utilize information-based metrics have been explored in the literature [10], [11]. Machine learning techniques for sensor placement aim to achieve efficient sensing with the fewest possible sensors and measurements [12]–[14]. Information-theoretic sensor placement methods employ performance metrics such as the Fisher information matrix (FIM) [15], entropy [16], Kullback-Leibler (KL) divergence [17], mutual information [18], [19] to maximize the amount of useful information collected from the environment. Although it is commonly studied in the mobile sensor network literature, the problem of accounting for sensor reconfiguration costs is relatively less studied for sensor placement. Reconfiguration cost becomes important when multiple iterations of the sensor configuration are implemented in a time-marching environment. Some prior research includes the reconfiguration cost of the sensor network topology [20], or the total energy consumption of the sensor network [21], [22].

*Graduate Research Assistant, Aerospace Engineering.

†Associate Professor, Aerospace Engineering, Worcester Polytechnic Institute, Worcester, MA, USA. Corresponding author.

II. PROBLEM FORMULATION

In this paper we consider the problem of optimal sensor configuration coupled with path-planning in an unknown dynamic environment. More specifically, the objective is to strategically place sensors in locations that provide information of the most relevance to the path-planning problem. For path-planning under uncertainty, the most relevant information is that which can maximally reduce uncertainty about the path cost. This is a relatively new research problem in that it departs from the usual separation of estimation and planning/control and instead explicitly couples sensor configuration to planning.

Earlier studies have addressed this problem in the context of static environments. A heuristic task-driven sensor placement approach called the interactive planning and sensing (IPAS) for static environments is reported in [23]. This approach is reported to outperform several decoupled sensor placement strategies by reducing the number of configurations necessary to achieve near-optimal paths. Sensor configuration for both location and field-of-view has also been investigated for static fields [24]. Optimal sensor placement in a time-varying threat field that is based on optimizing a novel path dependent information measure, referred to as *context-relevant mutual information* (CRMI) is presented in our previous work [25]. A modified sensor placement method that maximizes a weighted sum of CRMI and a reward for reducing distances traveled by sensors is reported in [26].

All of this prior research [25], [26] is based on an iterative process that identifies the optimal sensor configuration, obtains the sensor measurements, updates the threat estimates, and plans path accordingly. This iterative process terminates when the path cost variance falls below a user-specified threshold. *Crucially, the ego vehicle is assumed to move only after the optimal path has been identified.* In other words, ego vehicle is assumed to “wait” at its initial location until this iterative process converges. Whereas this assumption is relevant for the preliminary development of the coupled sensor configuration and planning methods, it is not acceptable from a practical perspective in time-varying environments. Waiting at the initial location can make the planning outcome obsolete due to changes in the environment.

The novelty of this work is that we consider a situation where the ego vehicle moves simultaneously with the sensor configuration process. Therefore, we refer to the proposed technique as *actively coupled sensor configuration and path-planning* (A-CSCP). We consider the optimization of a new sensor configuration objective function that depends not only on CRMI and the distance traveled by sensors, but also on the relative distances between the sensors and the ego vehicle as it moves.

The rest of the paper is organized as follows. In Sec. II, we introduce the elements of the problem formulation. In Sec. III, we present the new objective function and the A-CSCP iterative algorithm. In Sec. IV, we present illustrative examples and comparative results, and conclude the paper in Sec. V with comments on future work.

Let \mathbb{R} be the set of real numbers, \mathbb{N} the set of natural numbers, and $\mathbf{I}_{(N)}$ the identity matrix of size N . For any $N \in \mathbb{N}$, let $[N]$ denote $\{1, 2, \dots, N\}$.

In a closed square region, $\mathcal{W} \subset \mathbb{R}^2$, referred to as the workspace, a mobile agent operates alongside a network of spatially distributed sensors. The workspace is divided into a grid of N_g uniformly spaced points, with each point assigned coordinates \mathbf{x}_i in a prespecified Cartesian coordinate axis system, for each $i \in N_g$. The distance between adjacent grid points is denoted by δ . The agent navigates this grid according to the “4-way adjacency rule”, which means movement is restricted to adjacent points in the upward, downward, leftward, and rightward directions. This navigation problem is framed as a graph search over a graph $\mathcal{G} = (V, E)$, where $V = [N_g]$ is the set of vertices, and E is the set of edges connecting geometrically adjacent vertices. Each vertex in V is uniquely associated with a grid point.

A *threat field*, denoted as $c : \mathcal{W} \times \mathbb{R}_{\geq 0} \rightarrow \mathbb{R}_{>0}$, is a time-varying scalar field that takes strictly positive values, indicating regions with higher intensity that are potentially hazardous and unfavorable. The ego vehicle is required to move from a start vertex $i_s \in V$ to a goal vertex $i_g \in V$, following a path $\boldsymbol{\pi} = \{i_0, i_1, \dots, i_L\}$, where $i_0 = i_s$ and $i_L = i_g$ for some $L \geq 1$. The ego vehicle is assumed to move at a constant speed, u_{ego} . Each transition between vertices incurs a cost that is determined by the threat field exposure. The cost associated with traversing adjacent grid points is denoted by a scalar function $g : E \times \mathbb{R}_{\geq 0} \rightarrow \mathbb{R}_{>0}$ defined as

$$g((i, j), t) = c(\mathbf{x}_j, t) \quad \text{for } (i, j) \in E. \quad (1)$$

The overall threat exposure $J(\boldsymbol{\pi})$ along the path is the sum of the edge transition costs, i.e., $J(\boldsymbol{\pi}) := \delta \sum_{\ell=1}^L g((i_{\ell-1}, i_\ell), \ell \Delta t_s)$. The main goal is to identify a path $\boldsymbol{\pi}^*$ with a minimum cost.

Because the threat field is unknown, it is necessary to estimate its values. To this end, a mobile sensor network of N_s sensors is deployed to measure the intensity of the threat field at various points. We assume that $N_s \ll N_g$, i.e., that we have a relatively small number of sensors available. Each sensor in the network is assumed to move at a constant speed $u_{\text{sen}} > u_{\text{ego}}$. The sensor measurements are denoted $\mathbf{z}(t; \mathbf{q}) = \{z_1(t; \mathbf{q}), z_2(t; \mathbf{q}), \dots, z_{N_s}(t; \mathbf{q})\}$. The sensors are positioned at specific grid points, and the set of grid points where sensors are located is called the *sensor configuration*, $\mathbf{q} = \{q_1, q_2, \dots, q_{N_s}\} \subset [N_g]$.

The threat field is represented by a parametric model of the form $c(\mathbf{x}, t) := 1 + \sum_{n=1}^{N_P} \theta_n(t) \phi_n(\mathbf{x}) = 1 + \boldsymbol{\Phi}^T(\mathbf{x}) \boldsymbol{\Theta}(t)$, where $\boldsymbol{\Phi}(\mathbf{x})$ is a vector of spatial basis functions, defined as $\boldsymbol{\Phi}(\mathbf{x}) := [\phi_1(\mathbf{x}) \dots \phi_{N_P}(\mathbf{x})]^T$. Here, N_P represents the number of parameters used to model the threat field. For each $n \in [N_P]$, $\phi_n(\mathbf{x})$ is modeled as a Gaussian function, $\phi_n(\mathbf{x}) := \exp(-(\mathbf{x} - \bar{\mathbf{x}}_n)^T (\mathbf{x} - \bar{\mathbf{x}}_n) / 2a_n)$. The constants $a_n \in \mathbb{R}_{>0}$ and $\bar{\mathbf{x}}_n \in \mathcal{W}$ are prespecified, ensuring that the combined regions of influence of the basis functions sufficiently cover the entire workspace \mathcal{W} . The time-varying

parameter $\Theta(t) := [\theta_1(t) \dots \theta_{N_P}(t)]^\top$ is unknown and is to be estimated using the sensor measurements \mathbf{z} .

The temporal evolution of the threat in discrete form is defined using the linear system dynamic model,

$$\Theta_k = A\Theta_{k-1} + \omega_{k-1}, \quad (2)$$

where the matrix A represents some known evolution of threat parameters and $\omega_k \sim \mathcal{N}(0, Q)$, with $Q := \sigma_P \mathbf{I}_{(N_P)}$ for each $k \in \mathbb{N}$. In this paper we assume that the system (2) is stable.

The measurements obtained from each sensor are modeled by $\mathbf{z}_k := c(\mathbf{x}_{q_k}, t) + \boldsymbol{\eta}_k = H_k(\mathbf{q})\Theta_k + \boldsymbol{\eta}_k$, where the matrix

$$H_k(\mathbf{q}) = \begin{bmatrix} \Phi(\mathbf{x}_{q_{k,1}}) & \Phi(\mathbf{x}_{q_{k,2}}) & \dots & \Phi(\mathbf{x}_{q_{k,N_s}}) \end{bmatrix}^\top,$$

and $\boldsymbol{\eta}_k \sim \mathcal{N}(0, R)$ is zero mean measurement noise with covariance $R \succ 0$. Using these measurements and a Bayesian estimation algorithm such as the Kalman filter, we can find stochastic estimates of the threat parameter with mean value $\hat{\Theta}(t)$ and estimation error covariance P .

For any path, $\boldsymbol{\pi} = \{i_0, i_1, \dots, i_L\}$ in \mathcal{G} , the cost of the path is

$$J(\boldsymbol{\pi}) := L + \delta \sum_{\ell=1}^L \Phi^\top(\mathbf{x}_\ell) \Theta(t).$$

The cost J becomes a random variable with distribution dependent on the estimate Θ . The problem of interest in this paper is then defined as follows.

Problem 1. *For a prespecified ego vehicle start and goal vertices $i_s, i_g \in V$, with the ego vehicle and finite sensors moving at constant speeds u_{ego} and u_{sen} respectively, find sensor configurations \mathbf{q}^* and a path $\boldsymbol{\pi}^*$ with minimum expected threat exposure $\mathbb{E}[J(\boldsymbol{\pi}^*)]$.*

Because the number of sensors N_s is small relative to the number of grid points N_g , we seek an iterative solution to Problem 1, whereby the sensor configuration and planned path are iteratively updated. These iterations occur while the ego vehicle moves, and therefore the iterative computations must incorporate the ego vehicle's changing location.

III. ACTIVE COUPLED SENSING AND PLANNING

Active coupled sensor configuration and path-planning (A-CSCP) is the proposed approach to solve Problem 1 in a time-varying environment. At each time step, multiple sensors and an ego vehicle move at constant speeds towards their objectives. The sensors gather pointwise measurements of the threat field. The optimal sensor configuration is determined based on an information measure called *context-relevant mutual information* (CRMI), which we describe in further detail below. As each sensor reaches its next configuration, it takes a measurement and reports to a central server, which in turn updates the threat field estimate. Then, the optimal path for the ego vehicle is updated and a new configuration for the sensor is determined.

Any estimator can be employed to estimate the state parameters. If the threat parameter model is linear, as we assume in (2), then we may use a simple Kalman filter. For

generality and applicability to future work with nonlinear evolution models, we may utilize an Unscented Kalman Filter (UKF [8]).

As the ego vehicle travels and arrives at each grid point along its planned path, it replans its path based on the latest threat estimate. This coordinated interaction between sensor reconfiguration and ego vehicle movement provides continuous adaptation to the evolving threat environment. This process continues until the ego vehicle reaches the goal vertex. In what follows, we provide details of this iterative process, analysis, and an illustrative example.

A. Context Relevant Mutual Information

We define the *context-relevant mutual information* (CRMI) to quantify the information shared between the path cost and sensor measurements. CRMI is the novel and crucial coupling between sensor configuration and path-planning. The CRMI becomes maximum at the spatial locations of most relevance to path-planning, disregarding areas that are far from the intended path. In other words, placing sensors at maximum CRMI locations is likely to reduce the path cost uncertainty by the largest amount.

For any path $\boldsymbol{\pi}$, the expected cost is $\hat{J}(\boldsymbol{\pi}) := L + \delta \sum_{\ell=1}^L \Phi(\mathbf{x}_\ell)^\top \hat{\Theta}(t)$. Because the estimate $\hat{\Theta}$, P is Gaussian and because the path cost is a linear function of the parameter estimate, the path cost r.v. is also Gaussian. Therefore, the joint PDF $p(J_k, \mathbf{z}_k)$ of the path cost and measurement is

$$p(J_k, \mathbf{z}_k) = \mathcal{N} \left(\begin{bmatrix} J_k \\ \mathbf{z}_k \end{bmatrix} : \begin{bmatrix} \hat{J}_{k|k-1} \\ \hat{\mathbf{z}}_k \end{bmatrix}, \begin{bmatrix} P_{JJ_{k|k-1}} & P_{J\mathbf{z}_{k|k-1}} \\ P_{J\mathbf{z}_{k|k-1}}^\top & P_{\mathbf{z}\mathbf{z}_{k|k-1}} \end{bmatrix} \right).$$

The variance of the path cost is

$$\begin{aligned} P_{JJ_{k|k-1}} &:= \mathbb{E} \left[\left(J(\boldsymbol{\pi}) - \hat{J}(\boldsymbol{\pi}) \right)^2 \right] \\ &= \mathbb{E} \left[\left(\delta \sum_{\ell=1}^L \Phi^\top(\mathbf{x}_\ell) \left(\Theta(t) - \hat{\Theta}(t) \right) \right)^2 \right], \\ &= \delta^2 \sum_{\ell=1}^L \left(\Phi(\mathbf{x}_\ell)^\top P_{k\ell} \Phi(\mathbf{x}_\ell) \right) \\ &\quad + 2\delta^2 \sum_{\ell < m, \ell, m \in [L]} \left(\Phi(\mathbf{x}_\ell)^\top P_{k\ell m} \Phi(\mathbf{x}_m) \right). \quad (3) \end{aligned}$$

To compute $P_{JJ_{k|k-1}}$, we first need to determine Φ and the error covariance P for each grid point $\boldsymbol{\pi}_l$ along the path. P_{k_l} and $P_{k_{lm}}$ are determined by propagating the UKF prediction steps for a time steps for traversing between grid points. The covariance of the measurement and the cross covariance between the path cost and the measurement random vector are then formulated as

$$\begin{aligned} P_{J\mathbf{z}_{k|k-1}} &:= \mathbb{E} \left[(\mathbf{z} - \hat{\mathbf{z}}) \left(J(\boldsymbol{\pi}) - \hat{J}(\boldsymbol{\pi}) \right) \right] \\ &= \delta \sum_{l=1}^L \left(\Phi(\mathbf{x}_{\boldsymbol{\pi}_l})^\top P_{k_l} \right) H_k^\top(\mathbf{q}), \quad (4) \end{aligned}$$

$$P_{\mathbf{z}\mathbf{z}_{k|k-1}} = H_k(\mathbf{q}) P_{\Theta\Theta_{k|k-1}} H_k^\top(\mathbf{q}) + R_k. \quad (5)$$

Here, $P_{\Theta_{k|k-1}}$ is the priori state covariance that is obtained from the UKF algorithm. Finally, the CRMI is calculated as

$$I(J_k; \mathbf{z}_k(\mathbf{q})) = \frac{1}{2} \log \left(\frac{|P_{JJ_{k|k-1}}|}{|P_{JJ_{k|k-1}} - P_{J\mathbf{z}_{k|k-1}} P_{\mathbf{z}\mathbf{z}_{k|k-1}}^{-1} P_{J\mathbf{z}_{k|k-1}}^\top|} \right). \quad (6)$$

B. Sensor Reconfiguration Cost

In a previous work [25], we showed that CRMI is a submodular function. Optimization of submodular functions is computationally convenient because a greedy algorithm is known to converge to a near-optimal solution with bounded worst-case suboptimality [27]. In the present context, greedy optimization implies that we find the optimal configuration of each sensor one at a time. Based on this observation from previous work, we consider greedy optimization, only, in the rest of this work.

Sensor reconfiguration cost represents the cost associated with relocating mobile sensors within the environment. In this context, we define the sensor reconfiguration cost based on two distance components, described as follows.

At the ℓ^{th} sensor configuration within the A-CSCP algorithm (described in the next subsection) and for the j^{th} sensor, the first component, denoted d_1 , is the Euclidean distance between the sensor's current location $q_j^{\ell*}$ and its new candidate location $q_j^{\ell+1} \in [N_g] \setminus \mathbf{q}^{\ell*}$, i.e.,

$$d_1(q_j^{\ell+1}) := \|q_j^{\ell+1} - q_j^{\ell*}\|.$$

The second component d_2 is the distance between the sensor's new candidate location $q_j^{\ell+1}$ and the position $\mathbf{x}_{\text{ego}}^\ell$ of the ego vehicle's next planned grid point, i.e.,

$$d_2(q_j^{\ell+1}) = \|q_j^{\ell+1} - \mathbf{x}_{\text{ego}}^{\ell+1}\|.$$

In other words, $\mathbf{x}_{\text{ego}}^{\ell+1} \in \mathcal{W}$ is the location associated with the second vertex in the path planned at iteration ℓ . Considering this distance in the sensor reconfiguration cost allows the sensor placement to consider the proximity of the sensors to the ego vehicle.

Next, we define the weighted sum

$$d(q_j^{\ell+1}) := \gamma d_1(q_j^{\ell+1}) + (1 - \gamma) d_2(q_j^{\ell+1}).$$

The constant γ provides a trade-off between the two distance components d_1 and d_2 in the sensor reconfiguration cost. When $\gamma = 1$, the sensor configuration cost is solely based on the Euclidean distances traveled by the sensors. Similarly, when $\gamma = 0$, the sensor configuration cost considers the distance between sensor's current location and the ego vehicle next planned location, only.

Next, we define the sensor reconfiguration cost as

$$f(q_j^{\ell+1}) := \min_{q \in [N_g] \setminus \mathbf{q}^{\ell*}} \{d(q)\} - d(q_j^{\ell+1}). \quad (7)$$

Finally, we define the reward function

$$r(q_j^{\ell+1}) := I(J; \mathbf{z}(q_j^{\ell+1})) + \alpha f(q_j^{\ell+1}) \quad (8)$$

to be maximized for finding the next configuration for sensor j . Note that, due to the min term in (7), f is always

nonpositive, i.e., f reduces the reward associated with CRMI. In other words, r is a reward that encodes a balance between the most path-relevant informativeness, distance traveled by sensors, and proximity between sensors and the ego vehicle. The term $I(J; \mathbf{z}(q_j^{\ell+1}))$ is to be understood as the CRMI for the sensor configuration obtained by moving the j^{th} sensor to $q_j^{\ell+1}$ while keeping all other sensors fixed.

The next sensor configuration is then determined as

$$q_j^{(\ell+1)*} := \max_{q \in [N_g] \setminus \mathbf{q}^{\ell*}} \{r(q)\}. \quad (9)$$

The constant α in (8) is a normalizing factor that balances the trade-off between maximizing the CRMI metric and minimizing the sensor reconfiguration cost. To be precise:

$$\alpha := \frac{\max_q \{I(J; \mathbf{z}(q))\}}{\max_q \{d(q)\} - \min_q \{d(q)\}}. \quad (10)$$

The two maxima and the minimum in (10) are calculated over the set of feasible configurations $[N_g] \setminus \mathbf{q}^{\ell*}$.

C. Active CSCP Algorithm

Algorithm 1: A-CSCP Algorithm

- 1 Set time step $k = 0$, and $\widehat{\Theta}_0 = \mathbf{0}$, and $P_0 = \chi \mathbf{I}_{(N_P)}$
 - 2 Initialize sensor configuration $\mathbf{q}^{0*} \subset [N_g]$
 - 3 Initialize ego vehicle location to i_s
 - 4 Obtain $\mathbf{z}(t_0; \mathbf{q}^{0*})$ and update $\widehat{\Theta}_0, P_0$
 - 5 Find $\pi_0^* = \arg \min(\widehat{J}_0(\pi))$
 - 6 For each $j \in [N_s]$, find optimal sensor configuration $q_j^{1*} := \arg \max_q (r(q))$
 - 7 **while** ego vehicle position $\neq (\mathbf{x}_{i_g})$ **do**
 - 8 Move ego vehicle along π^* at speed u_{ego}
 - 9 **if** ego vehicle position is at (\mathbf{x}_{i_0}) **then**
 - 10 $i_0 = i_1$
 - 11 **end**
 - 12 **for** $j = 1 : N_s$ **do**
 - 13 Move sensor j toward $\mathbf{x}_{q_j^{\ell+1}}$ at speed u_{sen}
 - 14 **if** sensor j position is $\mathbf{x}_{q_j^{\ell+1}}$ **then**
 - 15 $\ell = \ell + 1$
 - 16 Obtain $\mathbf{z}_{t_\ell; \mathbf{q}^{\ell*}}$ and update $\widehat{\Theta}_k, P_k$
 - 17 Find $\pi_k^* = \arg \min(\widehat{J}_k(\pi))$
 - 18 Find optimal sensor configuration $q_j^{\ell*} = \arg \max_q (r(q))$
 - 19 **end**
 - 20 **end**
 - 21 $k = k + 1$
 - 22 **end**
-

The active coupled sensing and planning (A-CSCP) algorithm described in Algorithm 1 initializes with the prior $\widehat{\Theta}_0 = \mathbf{0}$ and $P_0 = \chi \mathbf{I}_{(N_P)}$, where χ is a large arbitrary number. The ego vehicle's start vertex is set as i_s , and the final goal vertex is i_g . The initial sensor configuration \mathbf{q}^{0*} is such that the sensors are placed at the immediate neighbors of i_s . The sensors immediately take measurements, and update

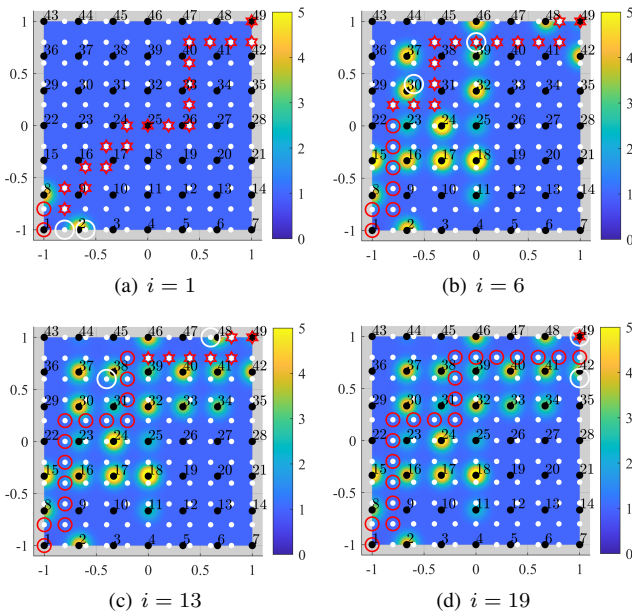


Fig. 1. Visualization of A-CSCP process for $N_P = 49$ and $N_g = 121$.

the estimates of Θ . An optimal path $\pi_0^* = \{i_0, i_1, \dots, i_L\}$ for the ego vehicle is determined (with $i_0 = i_s$), and the sensors then calculate their next configuration q^{1*} , using the aforesaid greedy method.

The ego vehicle and sensors then move at predefined speeds u_{ego} and u_{sen} , respectively toward their respective next vertices. When the ego vehicle reaches the next vertex, it adopts the latest optimal path, which is determined using the most recent threat field estimates based on the latest sensor measurements. The ego vehicle's starting vertex is updated to the next vertex, i_1 along the optimal path. Since the CRMI for the portion of the path already traversed is irrelevant for future path planning, the searching algorithm is restricted to considering only the relevant future paths, meaning that the previously traveled path cannot be altered.

For each sensor, the optimal sensor configuration is determined by maximizing the reward r defined in (8). When a sensor reaches its next configuration vertex, it takes a new measurement and the threat parameter estimate Θ is updated. Again a optimal path is calculated, and the new configuration for that sensor is determined. This process continues until the ego vehicle reaches the goal vertex i_g .

IV. RESULTS AND DISCUSSION

This section first provides an illustrative example of the proposed A-CSCP method. Next, we perform comparative analysis based on different schemes of sensor placement discussed earlier. All numerical simulations are performed within a square workspace $\mathcal{W} = [-1, 1] \times [-1, 1]$ using non-dimensional units.

A. Illustrative Example

An illustrative example of the A-CSCP algorithm with $\gamma = 1$ is presented in Fig. 1. Recall that with $\gamma = 1$ the sensor

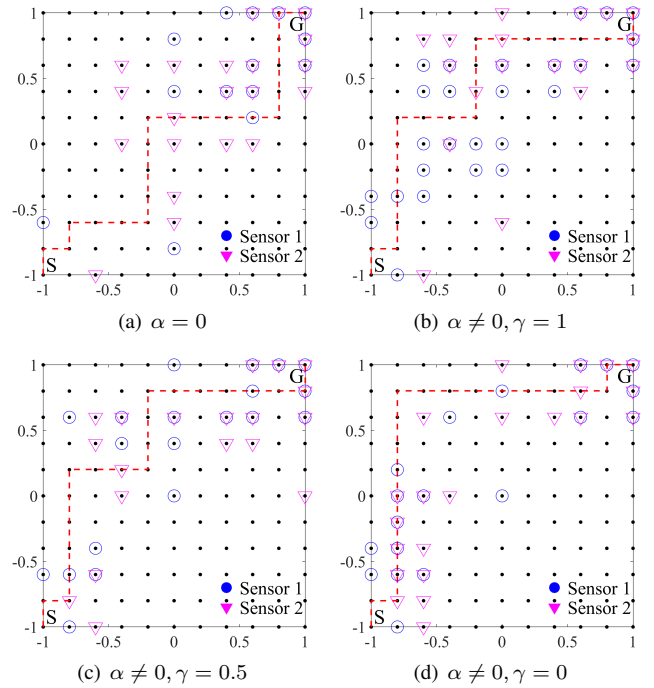


Fig. 2. Illustration of ego vehicle's path and sensor history for different sensor configuration schemes.

reconfiguration cost considers only the d_1 component. The number of threat parameters, grid points, and sensors are $N_P = 49$, $N_g = 121$, and $N_s = 2$, respectively. The threat parameters N_P , indicated by the black dots and numbered from 1 to 49, are uniformly spaced in the workspace. The white dots represent the grid points, whereas the white circles indicate sensor locations. The start and goal locations are the bottom left and the top right grid points, respectively. The ego vehicle moves at a constant speed of 0.01 and both sensors move at a constant speed of 0.05, such that $\frac{u_{sen}}{u_{ego}} = 5$.

The evolution of the threat field estimate \hat{c} and the path progression of the ego vehicle at different reached vertices, namely $i = 1, 6, 13$, and 19 is shown in a color map, where i is the number of vertices traveled by the ego vehicle along the path. The path traveled by the ego vehicle is represented by red circles, while the red stars indicate the planned future path. The planned path may be updated when new threat estimates become available. For $i = 1$, a path is planned based on only the initial sensor measurements. As the vehicle reaches each vertex along the path, the next vertex is chosen based on the latest estimate of the threat field provided by the sensors. This progression is illustrated in Fig. 1 (b), (c) and (d).

B. Comparative Study

For a comparative analysis, we implement via numerical simulation the A-CSCP method on the same threat field as in Fig. 1 by varying the type of reward function r used for finding the optimal sensor configurations.

In these simulations we record not only the cost J incurred by the ego vehicle as it moves from one grid point to the

next, but also the *total* exposure to the threat while traveling between the vertices.

Specifically, we record the *incurred cost*

$$\mathcal{J} := \int_{\pi} \Phi^T(\mathbf{x}(t)) \Theta(t) dt, \quad (11)$$

where \int_{π} is understood as the integral along a smooth curve interpolated over the grid points in the path π .

For the sake of analyzing the quality of the path eventually followed by the ego vehicle due to the proposed A-CSCP algorithm, consider two other benchmark paths for comparison: the worst-case path π^w and the true optimal π^t . Both of these benchmark paths are found assuming complete a priori knowledge of the threat field (which the A-CSCP does not have). The worst-case path π^w is chosen such that it passes through every peak of the threat field. The true optimal path π^t is easily calculated using Dijkstra's algorithm with complete knowledge of the threat field. Note that, the path length for π^w is same as of π^t . Let \mathcal{J}^w and \mathcal{J}^t denote the incurred costs of the worst-case and true optimal paths, respectively.

During the execution of the A-CSCP algorithm, we record the sensor configurations and specifically we record the number of *unique* grid point locations at which sensors are placed. Let S and U denote the total number and the unique number of grid points, respectively, at which sensors are placed throughout the execution of A-CSCP.

An efficiency measure η is defined as follows based on the ego vehicle's total threat exposure \mathcal{J} and the number of sensor placement locations:

$$\eta := \left(\frac{\mathcal{J}^w - \mathcal{J}}{\mathcal{J}^w - \mathcal{J}^t} \right) \frac{U}{S}. \quad (12)$$

This efficiency compares the incurred cost of the A-CSCP resultant path to that of the worst-case path, normalized by the difference between the worst-case and optimal incurred costs. η also incorporates a measure of efficiency in sensor motion, in that the efficiency is higher with fewer repeated placements of sensors at the same grid points.

The first comparative reconfiguration scheme utilizes CRMI metric, and $\alpha = 0$, which neglects any sensor placement costs. The other schemes consider the placement metrics that include f , with different values of γ , namely $\gamma = 1, 0.5$, and 0 .

Figure 2 depicts the total path taken by the ego vehicle as well as the vertices visited by each sensor. For $\alpha = 0$, the sensors have a tendency to travel farther between successive configurations, thereby taking fewer measurements by the time ego vehicle reaches the goal. This can be seen when comparing the S values from Table II. Furthermore, some grid locations have inherently higher MI values such as the goal, so there is a tendency to frequently visit these locations. The result of these two factors is evident in Fig. 2(a). The effect of the different placement schemes may be visually compared visually. For example, Figure 2(d) shows how the sensors strictly adhere to the path and rarely deviate, where

Figure 2(b) shows a much larger portion of the threat field being explored.

Table I provides the ego vehicle's normalized threat exposure. To compute the normalized values, the benchmark incurred costs \mathcal{J}^t and \mathcal{J}^w are assigned normalized scores of 1 and 0, respectively. That is, normalized values close to 1 indicate near-optimality. The schemes are tested for different sensor to ego vehicle speed ratios. The sensor speed will inherently impact the threat field exploration. For example, if the sensor speed is much greater than the ego vehicle speed, there is ample time for more of the threat field to be explored, and the sensor reconfiguration scheme becomes trivial. Table II shows for $\frac{u_{sen}}{u_{ego}} = 5$ the values of S and U recorded regarding sensor efficiency and the efficiency measure η as defined in (12). A scheme that finds the optimal path without the sensors revisiting any vertices achieves $\eta = 1$. The inclusion of f always increases η , with $\gamma = 1$ performing the best.

TABLE I
NORMALIZED THREAT EXPOSURE (\mathcal{J})

$\frac{u_{sen}}{u_{ego}}$	CRMI ($\alpha = 0$)	CRMI + Cost ($\alpha \neq 0$)		
		$\gamma = 1$	$\gamma = 0.5$	$\gamma = 0$
5	0.8712	0.9948	0.8974	0.9384
10	0.9064	0.9948	0.9841	0.9917
50	1	1	0.9948	1

TABLE II
EFFICIENCY METRIC (η)

	CRMI ($\alpha = 0$)	CRMI + Cost ($\alpha \neq 0$)		
		$\gamma = 1$	$\gamma = 0.5$	$\gamma = 0$
S	69	89	75	83
U	27	34	29	29
η	0.3409	0.3800	0.3470	0.3278

V. CONCLUSIONS

In this paper, we presented a technique for simultaneously sensing and planning for an ego vehicle moving at a constant speed, accompanied by multiple sensors also moving at constant speeds. The sensor placement is based on maximizing a reward that includes uncertainty reduction in the path cost and reduction in sensor movement. A sensor reconfiguration cost is considered for reducing the distance traveled by sensors between configurations while ensuring that the sensors remain in proximity to the ego vehicle. Numerical simulations are performed on different schemes of sensor placement metric and various sensor to ego vehicle speed ratios. The performance efficiency of the different schemes is evaluated based on the total threat exposure and the number of sensor configurations during the A-CSCP process. Based on the defined performance metric, the sensor placement scheme that maximizes the CRMI metric while minimizing

the sensor travel distance between successive configurations performs better in terms of an efficiency measure.

ACKNOWLEDGMENTS

This work is funded in part by NSF grant #2126818.

REFERENCES

- [1] S. M. LaValle, *Planning Algorithms*. Cambridge University Press, 2006.
- [2] B. K. Patle, G. B. L. A. Pandey, D. R. Parhi, and A. Jagadeesh, "A review: On path planning strategies for navigation of mobile robot," *Defence Technology*, vol. 15, pp. 582–606, August 2019.
- [3] T. Wen, X. Wang, Z. Zheng, and Z. Sun, "A DRL-based path planning method for wheeled mobile robots in unknown environments," *Computers and Electrical Engineering*, vol. 118, p. 109425, 2024.
- [4] Y. Qin, Z. Zhang, X. Li, W. Huangfu, and H. Zhang, "Deep reinforcement learning based resource allocation and trajectory planning in integrated sensing and communications UAV network," *IEEE Transactions on Wireless Communications*, vol. 22, no. 11, pp. 8158–8169, 2023.
- [5] F. L. Lewis, L. Xie, and D. Popa, *Optimal and robust estimation: with an introduction to stochastic control theory*. CRC press, 2017.
- [6] I. J. Myung, "Tutorial on maximum likelihood estimation," *Journal of mathematical Psychology*, vol. 47, no. 1, pp. 90–100, 2003.
- [7] S. Thrun, W. Burgard, and D. Fox, *Probabilistic Robotics*. The MIT Press, 2006.
- [8] S. J. Julier and J. K. Uhlmann, "Unscented filtering and nonlinear estimation," in *Proceedings of the IEEE*, vol. 92, pp. 401–422, Mar. 2004.
- [9] X. Deng, A. Mousavian, Y. Xiang, F. Xia, T. Bretl, and D. Fox, "PoseRBPF: A Rao–Blackwellized particle filter for 6-D object pose tracking," *IEEE Transactions on Robotics*, vol. 37, no. 5, pp. 1328–1342, 2021.
- [10] A. Kohara, K. Okano, K. Hirata, and Y. Nakamura, "Sensor placement minimizing the state estimation mean square error: Performance guarantees of greedy solutions," in *2020 59th IEEE Conference on Decision and Control (CDC)*, pp. 1706–1711, IEEE, 2020.
- [11] A. A. Soderlund and M. Kumar, "Optimization of multitarget tracking within a sensor network via information-guided clustering," *Journal of Guidance, Control, and Dynamics*, vol. 42, pp. 317–334, Feb. 2019.
- [12] P. Nayak, G. Swetha, S. Gupta, and K. Madhavi, "Routing in wireless sensor networks using machine learning techniques: Challenges and opportunities," *Measurement*, vol. 178, p. 108974, 2021.
- [13] Z. Wang, H. X. Li, and C. Chen, "Reinforcement learning-based optimal sensor placement for spatiotemporal modeling," *IEEE Transactions on Cybernetics*, vol. 50, pp. 2861–2871, Jun. 2020.
- [14] F. Hoffmann, A. Charlish, M. Ritchie, and H. Griffiths, "Sensor path planning using reinforcement learning," in *IEEE 23rd International Conference on Information Fusion (FUSION)*, pp. 1–8, 2020.
- [15] T. Kangsheng and Z. Guangxi, "Sensor management based on fisher information gain," *Journal of Systems Engineering and Electronics*, vol. 17, pp. 531–534, 2006.
- [16] H. Wang, K. Yao, G. Pottie, and D. Estrin, "Entropy-based sensor selection heuristic for target localization," in *3rd Int. Symp. Information Processing in Sensor Networks*, pp. 36–45, Apr. 2004.
- [17] S.-J. Liu, W. H. Lam, M. L. Tam, H. Fu, H. Ho, and W. Ma, "Network-wide speed–flow estimation considering uncertain traffic conditions and sparse multi-type detectors: A kl divergence-based optimization approach," *Transportation Research Part C: Emerging Technologies*, vol. 169, p. 104858, 2024.
- [18] A. Krause, A. Singh, and C. Guestrin, "Near-optimal sensor placements in gaussian processes: Theory, efficient algorithms and empirical studies," *Journal of Machine Learning Research*, vol. 9, pp. 235–284, 2008.
- [19] N. Adurthi, P. Singla, and M. Majji, "Mutual information based sensor tasking with applications to space situational awareness," *Journal of Guidance, Control, and Dynamics*, vol. 43, pp. 767–789, Apr. 2020.
- [20] A. S. Leong, D. E. Quevedo, A. Ahlén, and K. H. Johansson, "Network topology reconfiguration for state estimation over sensor networks with correlated packet drops," *IFAC Proceedings Volumes*, vol. 47, no. 3, pp. 5532–5537, 2014.
- [21] G. S. Ramachandran, W. Daniels, N. Matthys, C. Huygens, S. Michiels, W. Joosen, J. Meneghello, K. Lee, E. Canete, M. D. Rodriguez, *et al.*, "Measuring and modeling the energy cost of reconfiguration in sensor networks," *IEEE Sensors Journal*, vol. 15, no. 6, pp. 3381–3389, 2015.
- [22] H. Gricchi, O. Mosbahi, M. Khalgui, and Z. Li, "New power-oriented methodology for dynamic resizing and mobility of reconfigurable wireless sensor networks," *IEEE Transactions on Systems, Man, and Cybernetics: Systems*, vol. 48, no. 7, pp. 1120–1130, 2017.
- [23] B. S. Cooper and R. V. Cowlagi, "Interactive planning and sensing in unknown static environments with task-driven sensor placement," *Automatica*, vol. 105, pp. 391–398, Jul. 2019.
- [24] C. S. Laurent and R. V. Cowlagi, "Near-optimal task-driven sensor network configuration," *Automatica*, vol. 152, Jun. 2023.
- [25] P. Poudel and R. V. Cowlagi, "Coupled sensor configuration and planning in unknown dynamic environments with context-relevant mutual information-based sensor placement," in *2024 American Control Conference (ACC)*, pp. 306–311, IEEE, 2024.
- [26] P. Poudel and R. V. Cowlagi, "Reconfiguration costs in coupled sensor configuration and path-planning for dynamic environments," in *AIAA Scitech 2025 Forum*, (Orlando, Florida), 6–10 January 2025. to appear.
- [27] G. L. Nemhauser, L. A. Wolsey, and M. L. Fisher, "An analysis of approximations for maximizing submodular set functions—I," *Mathematical programming*, vol. 14, pp. 265–294, 1978.